

Band structure renormalization and weak pseudogap behavior in $\text{Na}_{0.33}\text{CoO}_2$: Fluctuation exchange study based on a single band model

Zi-Jian Yao,^{1,2} Jian-Xin Li,¹ and Z. D. Wang^{2,1}

¹National Laboratory of Solid State Microstructures and Department of Physics, Nanjing University, Nanjing 210093, China

²Department of Physics and Center of Theoretical and Computational Physics, The University of Hong Kong, Pokfulam Road, Hong Kong, China

(Dated: November 28, 2018)

Based on a single band Hubbard model and the fluctuation exchange approximation, the effective mass and the energy band renormalization in $\text{Na}_{0.33}\text{CoO}_2$ is elaborated. The renormalization is observed to exhibit certain kind of anisotropy, which agrees qualitatively with the angle-resolved photoemission spectroscopy (ARPES) measurements. Moreover, the spectral function and density of states (DOS) in the normal state are calculated, with a weak pseudogap behavior being seen, which is explained as a result of the strong Coulomb correlations. Our results suggest that the large Fermi surface (FS) associated with the a_{1g} band plays likely a central role in the charge dynamics.

PACS numbers: 74.70.-b, 71.18.+y, 71.27.+a, 74.25.Jb

The layered oxide Na_xCoO_2 has attracted much attention due to its possible connection to the high- T_c superconductivity since the discovery of superconductivity in it.^{1,2} This material consists of two-dimensional CoO_2 layers, where Co's form a triangular lattice, making the Na_xCoO_2 a possible realization of Anderson's resonating valence bond (RVB) state.³ By hydration, it becomes a superconductor with $T_c \approx 5\text{K}$ in $\text{Na}_{0.337}\text{CoO}_2 \cdot 1.3\text{H}_2\text{O}$ ¹. The unhydrated compound Na_xCoO_2 exhibits a rich phase diagram: a paramagnetic metal ($x < 0.5$), a charge-ordered insulator ($x = 0.5$), a "Curie-Weiss metal" ($x \sim 0.7$), and a magnetic order state ($x \geq 0.75$).⁴

Experimentally, it is indicated that Na_xCoO_2 seems to be strongly electronic correlated.^{2,5,6} Angle-resolved photoemission spectroscopy (ARPES) measurements show a strong mass renormalization (The effective mass is about 5-10 times larger than the bare mass.) for $x = 0.6$.⁷ Decreasing the Na concentration to $x = 0.3$, the cobaltates appear to be less electron-correlated with a weaker but still apparent energy band renormalization factor (~ 2).⁸ For the hydrated compounds, the effective mass is estimated to be $\sim 2 - 3$.⁹ In addition, recent experiments reported that $\text{Na}_{0.33}\text{CoO}_2 \cdot 1.3\text{H}_2\text{O}$ display certain pseudogap behaviors such as the decreasing of the Knight shift¹⁰ and the density of states (DOS) at the Fermi level below 300K.¹¹ Optical spectroscopy measurements for $\text{Na}_{0.2}\text{CoO}_2$ and $\text{Na}_{0.5}\text{CoO}_2$ also suggest the incipient formation of pseudogap.¹² However, unlike the pseudogap effect observed in the high- T_c cuprates, the pseudogap behavior is rather weak. The renormalization of the energy band and the pseudogap formation are directly related to the electronic structure, such as the quasiparticle spectral function, the quasiparticle dispersion, and the Fermi surface (FS) topology. Therefore it is of importance and significance to study the normal state quasiparticle dynamics.

It is believed that the topology of the FS plays an important role in the unconventional superconductivity. The local density approximation (LDA) calculations^{13,14}

predict a large FS associated with the a_{1g} band and six pockets associated with the e'_g band. However, intriguingly, the small pockets have not been observed in the ARPES measurements.^{8,9,15} The unexpected inconsistency of the topology of the FS between the LDA results and the ARPES measurements has aroused much controversy. One possibility might be due to the surface effect in the ARPES measurements. From another viewpoint, Zhou *et al.* suggested that the strong Coulomb interactions may induce significant renormalization of the band structure which pulls the e'_g band down from the Fermi energy.¹⁶ Furthermore, the e'_g band is suggested to be relevant to the spin-triplet superconductivity in some theoretical and numerical studies.^{17,18} On the other hand, the possibility of the spin-singlet superconductivity is also suggested according to recent Knight-shift measurements.^{19,20} Taking the above considerations into account, a single band model focusing on the a_{1g} band may be a starting point as a minimal model of Na_xCoO_2 .

In this paper, we study the normal state electronic structure in $\text{Na}_{0.33}\text{CoO}_2$ on the basis of the single band Hubbard model and the fluctuation exchange (FLEX) approximation. Several experimental features, such as the band renormalization and the weak pseudogap behavior, are well reproduced, which suggests an important role of the holelike Fermi surface centered around the Γ point in the quasiparticle dynamics. We start with the two-dimensional single band Hubbard model given by,

$$H = \sum_{ij,\sigma} (t_{ij} c_{i\sigma}^\dagger c_{j\sigma} + h.c.) + U \sum_i n_{i\uparrow} n_{i\downarrow} - \mu \sum_{i\sigma} n_{i\sigma} \quad (1)$$

where t_{ij} denotes the hopping term (in the following we will use t_1, t_2, t_3 and t_4 to denote the hoppings along the nearest- to the fourth nearest-neighbors), U the on-site Coulomb repulsion and μ the chemical potential. To reproduce the large FS around the Γ point, we set the parameters (t_1, t_2, t_3, t_4) of the bare dispersion $\epsilon_{\mathbf{k}}$ to be $(-1, 0, 0, 0.2)$, where t_1 is set to be the unit hereafter. According to the numerical result for the bandwidth,^{13,21}

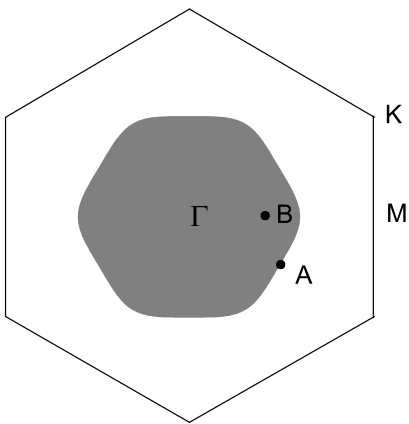


FIG. 1: The Fermi surface of $\text{Na}_{0.33}\text{CoO}_2$ for $(t_1, t_2, t_3, t_4) = (-1, 0, 0, 0.2)$. The grey area denotes the unoccupied electron states. Point A near the Fermi surface indicates the \mathbf{k} -point where m^* is calculated.

one can get $t_1 = 130$ meV. We note that the main feature of the bare dispersion is similar to that of the band with an a_{1g} character in the LDA calculation by Lee *et al.*¹⁴

The FLEX approximation is employed in our study, which has been applied to the two dimensional Hubbard model in literatures.^{22,23,24,25} As a self-consistent approximation, the FLEX approximation solves the Dyson's equation with a primarily RPA+ladder type effective interaction self-consistently. Based on the scenario of the FLEX approximation, the self-energy is given by,

$$\Sigma(k) = \frac{T}{N} \sum_q V_{eff}(k-q)G(q), \quad (2)$$

where

$$V_{eff}(q) = \frac{3}{2}U^2\chi_s(q) + \frac{1}{2}U^2\chi_c(q). \quad (3)$$

The spin susceptibility is

$$\chi_s(q) = \frac{\bar{\chi}(q)}{1 - U\bar{\chi}(q)}, \quad (4)$$

and the charge susceptibility is

$$\chi_c(q) = \frac{\bar{\chi}(q)}{1 + U\bar{\chi}(q)}, \quad (5)$$

with the irreducible susceptibility,

$$\bar{\chi}(q) = -\frac{T}{N} \sum_k G(k+q)G(k). \quad (6)$$

The electron Green's function is give by,

$$G(k) = [i\omega_n - \epsilon_k - \Sigma(k)]^{-1}. \quad (7)$$

In the above equations, $k \equiv (\mathbf{k}, i\omega_n)$ and $q \equiv (\mathbf{q}, i\nu_n)$ are used, T is the temperature. These equations are

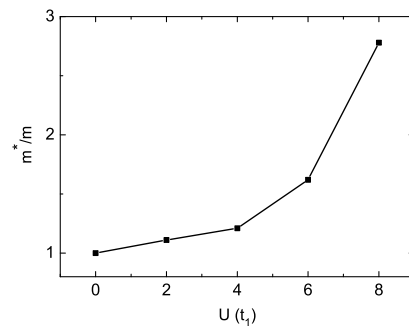


FIG. 2: The ratio of the effective mass to the bare mass m^*/m at point A as indicated in Fig. 1 versus the on-site Coulomb repulsion U at $T = 0.1$.

solved self-consistently, where $N = 64 \times 64$ \mathbf{k} -point meshes and up to 2048 Matsubara frequencies $\omega_n = (2n+1)\pi T$ are taken. The electron density is determined by the chemical potential μ from the equation $\langle n \rangle = 1 - \frac{2T}{N} \sum_k G(k)$.

As an important physical quantity related closely to the strength of the electronic correlations, the effective mass m^* is given by

$$\frac{m}{m^*} = Z \left(1 + \frac{m}{k_F} \frac{\partial}{\partial k} \text{Re} \Sigma(k, \omega) \Big|_{k=k_F} \right), \quad (8)$$

where

$$Z = \left(1 - \frac{\partial}{\partial \omega} \text{Re} \Sigma(k_F, \omega) \Big|_{\omega=0} \right)^{-1} \quad (9)$$

is the renormalization constant. The self-energy with real frequencies $\Sigma(\mathbf{k}, \omega)$ is obtained with the Padé approximants,²⁶ which analytically continue $\Sigma(\mathbf{k}, i\omega)$ from the Matsubara frequencies to the real-frequency axis. The ratio of the effective mass to the bare mass m^*/m with different on-site Coulomb repulsions U near the FS (point A in Fig. 1) is plotted in Fig. 2, where m^*/m increases monotonously with the increasing of U . It is noticeable that when U is less than 4, the enhancement of the effective mass is inapparent (< 1.2). With a strong Coulomb repulsion ($U \geq 6 \approx 0.8$ eV), the effective mass is enhanced significantly. Comparing the calculated effective mass with the ARPES measurements (~ 2 for $x \sim 0.3$), we set $U \sim 6$ in the present simple model to reflect the strong correlation effect in $\text{Na}_{0.33}\text{CoO}_2$.²⁷ The strong electronic correlations are evident from Fig. 3 (a), where the sharp quasiparticle peak is suppressed with strong Coulomb repulsion. For $U = 2$ and $T = 0.1$, the spectral function shows a sharp peak near the Fermi energy. Increasing the Coulomb repulsion to $U = 6$, the spectral function is broadened and the spectral weight at the Fermi level is reduced greatly.

For $U = 6$ we now investigate the renormalization of the quasiparticle energy band. To do it, we need to evaluate the spectral function of quasiparticles defined as

$$A(\mathbf{k}, \omega) = -\frac{1}{\pi} \text{Im} G(\mathbf{k}, \omega), \quad (10)$$

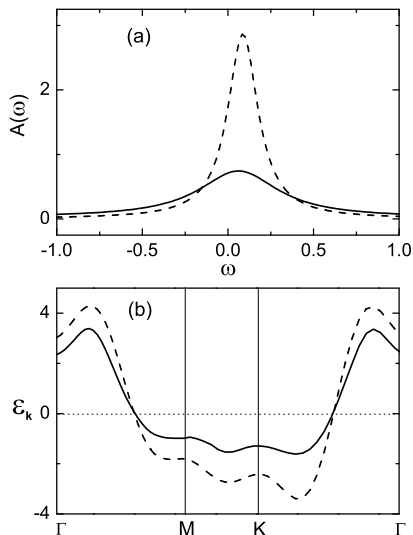


FIG. 3: (a) The effect of the on-site Coulomb repulsion on the spectral function at point A of Fig. 1. Solid line: $U = 6$, $T = 0.1$. Dashed line: $U = 2$, $T = 0.1$. (b) Solid line: the renormalized band dispersion for $U = 6$ and $T = 0.1$. Dashed line: the bare band dispersion. Dotted line: the Fermi energy.

where $G(\mathbf{k}, \omega)$ is the dressed Green's function in real frequency, which is analytically continued from the dressed Green's function in imaginary-frequency via the Padé approximants. Then, the renormalized band dispersion is determined by the position of the peak of $A(\mathbf{k}, \omega)$. The calculated result at $T = 0.1$ is shown in Fig. 3 (b), where the solid and the dotted lines denote the renormalized and the bare energy bands, respectively. One can see that the bandwidth is compressed obviously due to the strong Coulomb interactions. From Fig. 3 (b) we get the bandwidth of the bare band dispersion (7.7) and the renormalized bandwidth (5.0), which gives a band renormalization factor 1.54. This is consistent with the ARPES measurements for $x = 0.3$.⁸ Moreover, we find that the band renormalization shows an anisotropy along the Γ - K and Γ - M direction, namely the renormalization along the Γ - K direction is stronger than that along the Γ - M direction. The similar anisotropy has been found in the ARPES experiments for $x = 0.6$,⁷ though the experimental result seems stronger than what we disclosed here. We note that the compound Na_xCoO_2 with $x = 0.6$ is in fact in the range of the Curie-Weiss metal, in which the correlation is stronger than that in the paramagnetic metal with $x = 0.3$. So, a weaker anisotropy in the renormalization is expected. This anisotropy originates from the nesting of the Fermi surface along the Γ - K direction as shown in Fig. 1.

We now turn to address the weak pseudogap behavior. This is manifested in the suppression of the density of states at the Fermi level. We present the ω dependence of the density of states at different temperatures in Fig. 4. With the decrease of temperature from $T = 0.7$ (dash dotted) through $T = 0.5$ (dotted) and $T = 0.3$ (dashed)

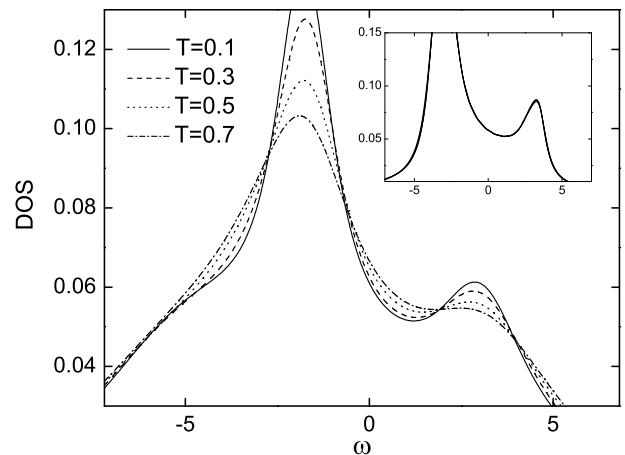


FIG. 4: The total density of states (DOS) versus energy for $U = 6$. Solid line: $T = 0.1$, dashed line: $T = 0.3$, dotted line: $T = 0.5$, and dash-dotted line: $T = 0.7$. Inset: DOS plots for $U = 2$ at $T = 0.1, 0.3, 0.5, 0.7$.

to $T = 0.1$ (solid), a weak suppression of the density of states near the Fermi energy is evident, suggesting the opening of a weak pseudogap. The weak pseudogap behavior is also manifested in the quasiparticle spectral function $A(\mathbf{k}, \omega)$ which measures the probability to find the quasiparticle at momentum \mathbf{k} and frequency ω . As shown in Fig. 5 (a), with the decrease of temperature (from the dashed line to the solid line), the spectral weight is transferred away from the region around $\omega = 0$, producing a weak secondary maximum at $\omega < E_F$. Thus, a weak pseudogap is formed.

This weak pseudogap behavior is a consequence of strong Coulomb repulsion. To show this, we also present the results with a smaller $U = 2$ at $T = 0.1, 0.3, 0.5, 0.7$ in the insert of Fig. 4. Different from the $U = 6$ case, the density of states is not suppressed with the decreasing of temperature at all (in fact there is no appreciable difference between them, so only one line can be seen from the figure). For a more detailed discussion, we also present the spectral function for $U = 2$ (dotted), $U = 4$ (dash dotted) and $U = 6$ (solid) in Fig. 5 (a), where the secondary maximum shows up gradually with the increase of the Coulomb correlations. Note that since the secondary maximum disappears for $U = 2$, no pseudogap is expected for this case and what for $U < 2$. We refer to the depression of the spectral weight to be a weak pseudogap here is based on the observation that the spectral function consists of a peak and a weak secondary maximum (not a peak). In fact, the real part of the denominator of the Green's function has only one pole, which can be seen from the real part of the self-energy shown in Fig. 5 (b). It is the extremum of the imaginary part of the self energy around $\omega = -4$ that produces the weak maximum of the spectral function, as shown in Fig. 5 (c). In the case of a smaller Coulomb repulsion U , such as $U = 2$, a usual Fermi-liquid form of the self-energy is preserved (The dotted lines in Fig. 5 (b) and (c)), so it gives a

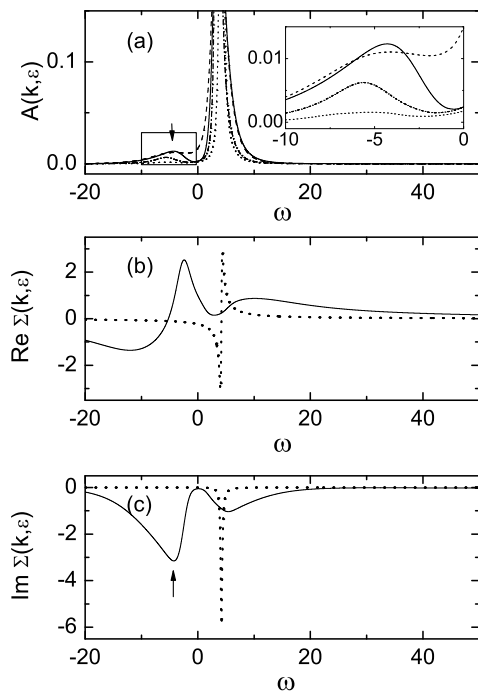


FIG. 5: (a) The energy dependence of the spectral function at the momentum indicated as point *B* in Fig. 1. Below the Fermi energy, there is a small peak in the spectral function for $U = 6$ and $T = 0.1$ (solid line). Dashed line: $U = 6$ and $T = 0.7$, dash-dotted line: $U = 4$, $T = 0.1$, dotted line: $U = 2$, $T = 0.1$. The arrow points to the location of the secondary maximum. Inset: Zoom-in view of the solid rectangle. (b) and (c): The real and the imaginary part of the self-energy at $T = 0.1$ for $U = 6$ (solid) and $U = 2$ (dotted). The arrow indicates the position of the extrema in $\text{Im } \Sigma(\mathbf{k}, \omega)$.

well defined quasiparticle peak in the spectral function (The dotted line in Fig. 5 (a)). This secondary maximum might suggest a "shadow band",²⁸ which occurs when a short-range spin correlation is developed with the increase of Coulomb repulsion. Therefore, the weak pseudogap behavior reported here may be due to the spin fluctuation in the strong correlated regime.²⁹

A similar weak pseudogap behavior was reported by Yada *et al.*³⁰ based on a multi-orbital model with the absence of small hole pockets. Our results based on the single band model provide further support for the sinking down of the small hole pockets. In our opinion, the agreement between the two models suggests that the multi-orbital effect may play a minor role in the mechanism of the pseudogap formation.

In summary, we have studied the quasiparticle band renormalization and the pseudogap behavior in $\text{Na}_{0.33}\text{CoO}_2$ based on the single band Hubbard model in a two-dimensional triangle lattice. The renormalization of the band structure and its anisotropy of the Γ - K and Γ - M direction have been elaborated. The estimated effective mass is consistent with the ARPES measurements. In the meantime, a weak pseudogap behavior is reproduced, which is explained as the result of the strong spin fluctuations. Our results are qualitatively consistent with experiments as well as the theoretical calculations based on a multi-orbital model.

We thank Q.-H. Wang for helpful discussions. The work was supported by the NSFC (10525415, 10474032, 10429401), the RGC grants of Hong Kong (HKU7045/04P, HKU-3/05C), and the State Key Program for Basic Research of China (2006CB921800, 2006CB601002).

- ¹ K. Takada, H. Sakurai, E. Takayama-Muromachi, F. Izumi, R. A. Dilanian, and T. Sasaki, *Nature (London)* **422**, 53 (2003).
- ² Y. Wang, N. S. Rogado, R. J. Cava, and N. P. Ong, *Nature (London)* **423**, 425 (2003).
- ³ G. Baskaran, *Phys. Rev. Lett.* **91**, 097003 (2003).
- ⁴ M. L. Foo, Y. Wang, S. Watauchi, H. W. Zandbergen, T. He, R. J. Cava, and N. P. Ong, *Phys. Rev. Lett.* **92**, 247001 (2004).
- ⁵ R. Jin, B. C. Sales, P. Khalifah, and D. Mandrus, *Phys. Rev. Lett.* **91**, 217001 (2003).
- ⁶ F. C. Chou, J. H. Cho, P. A. Lee, E. T. Abel, K. Matan, and Y. S. Lee, *Phys. Rev. Lett.* **92**, 157004 (2004).
- ⁷ H.-B. Yang, S.-C. Wang, A. K. P. Sekharan, H. Matsui, S. Souma, T. Sato, T. Takahashi, T. Takeuchi, J. C. Campuzano, R. Jin, et al., *Phys. Rev. Lett.* **92**, 246403 (2004).
- ⁸ H.-B. Yang, Z.-H. Pan, A. K. P. Sekharan, T. Sato, S. Souma, T. Takahashi, R. Jin, B. C. Sales, D. Mandrus, A. V. Fedorov, et al., *Phys. Rev. Lett.* **95**, 146401 (2005).
- ⁹ T. Shimojima, K. Ishizaka, S. Tsuda, T. Kiss, T. Yokoya, A. Chainani, S. Shin, P. Badica, K. Yamada, and K. Togano, *Phys. Rev. Lett.* **97**, 267003 (2006).
- ¹⁰ F. L. Ning, T. Imai, B. W. Statt, and F. C. Chou, *Phys. Rev. Lett.* **93**, 237201 (2004).
- ¹¹ T. Shimojima, T. Yokoya, T. Kiss, A. Chainani, S. Shin, T. Togashi, S. Watanabe, C. Zhang, C. T. Chen, K. Takada, et al., *Phys. Rev. B* **71**, 020505 (2005).
- ¹² J. Hwang, J. Yang, T. Timusk, and F. C. Chou, *Phys. Rev. B* **72**, 024549 (2005).
- ¹³ D. J. Singh, *Phys. Rev. B* **61**, 13397 (2000).
- ¹⁴ K.-W. Lee, J. Kunes, and W. E. Pickett, *Phys. Rev. B* **70**, 045104 (2004).
- ¹⁵ M. Z. Hasan, Y.-D. Chuang, D. Qian, Y. W. Li, Y. Kong, A. Kuprin, A. V. Fedorov, R. Kimmerling, E. Rotenberg, K. Rossnagel, et al., *Phys. Rev. Lett.* **92**, 246402 (2004).
- ¹⁶ S. Zhou, M. Gao, H. Ding, P. A. Lee, and Z. Wang, *Phys. Rev. Lett.* **94**, 206401 (2005).
- ¹⁷ K. Kuroki, Y. Tanaka, and R. Arita, *Phys. Rev. Lett.* **93**, 077001 (2004).
- ¹⁸ K. Kuroki, Y. Tanaka, and R. Arita, *Phys. Rev. B* **71**, 024506 (2005).
- ¹⁹ Y. Kobayashi, M. Yokoi, and M. Sato, *Journal of the Physical Society of Japan* **72**, 2453 (2003).
- ²⁰ G.-q. Zheng, K. Matano, D. P. Chen, and C. T. Lin, *Phys.*

- Rev. B **73**, 180503 (2006).
- ²¹ J. Kunes, K. W. Lee, and W. E. Pickett, *Charge disproportionation and spin-ordering tendencies in $na(x)coo_2$ at $x=1/3$* (2004), URL <http://www.citebase.org/abstract?id=oai:arXiv.org:cond-mat/0308388>.
- ²² P. Monthoux and D. J. Scalapino, Phys. Rev. Lett. **72**, 1874 (1994).
- ²³ C.-H. Pao and N. E. Bickers, Phys. Rev. Lett. **72**, 1870 (1994).
- ²⁴ T. Dahm and L. Tewordt, Phys. Rev. Lett. **74**, 793 (1995).
- ²⁵ Z.-J. Yao, J.-X. Li, and Z. D. Wang, Phys. Rev. B **74**, 212507 (2006).
- ²⁶ H. J. Vidberg and J. W. Serene, J. Low Temp. Phys. **29**, 179 (1977).
- ²⁷ Given $t_1 = U = 6t \approx 0.8eV$. We note that similar Hubbard U value has been used in other theoretical studies, see for example, K. Kuroki, S. Ohkubo, T. Nojima, R. Arita, S. Onari, and Y. Tanaka, Phys. Rev. Lett. **98**, 136401 (2007).
- ²⁸ J. J. Deisz, D. W. Hess, and J. W. Serene, Phys. Rev. Lett. **76**, 1312 (1996).
- ²⁹ We note that with stronger Coulomb repulsion, e.g., $U = 10$, no qualitative difference is found. However, as expected, the secondary-maximum-structure in $A(\mathbf{k}, \omega)$ becomes more obvious as well as the pseudogap effect.
- ³⁰ K. Yada and H. Kontani, Journal of the Physical Society of Japan **74**, 2161 (2005).